Journal of Surgical Research **149,** 310–318 (2008)
doi:10.1016/j.jss.2008.02.007

Assessment of Critical Renal Ischemia With Real-Time Infrared Imaging

Alexander M. Gorbach, Ph.D.,* Hengliang Wang, Ph.D.,† Nadeem N. Dhanani, M.D.,‡ Fred A. Gage,† Peter A. Pinto, M.D.,‡ Paul D. Smith, Ph.D.,* Allan D. Kirk, M.D., Ph.D.,§,[2] and Eric A. Elster, M.D.†,¶,‖,[1]

*Laboratory of Bioengineering and Physical Science, National Institute of Biomedical Imaging and Bioengineering, National Institutes of Health, Bethesda, Maryland; †Naval Medical Research Center, Silver Spring, Maryland; ‡Urologic Oncology Branch, National Cancer Institute, Bethesda, Maryland; §Transplant Branch, National Institute of Diabetes and Digestive and Kidney Diseases, Bethesda, Maryland; ¶Department of Surgery, National Naval Medical Center, Bethesda, Maryland; and ‖Department of Surgery, Uniformed Services University of the Health Sciences, Bethesda, Maryland

Submitted for publication December 11, 2007

Background. **Currently visual and tactile clues such as color, mottling, and tissue turgor are used in the operating room for subjective assessments of organ ischemia. Studies have demonstrated that infrared (IR) imaging is a reliable tool to identify perfusion of brain tumors and kidneys during human surgery. Intraoperative IR imaging has the potential for more objective real-time detection and quantitative assessment of organ viability including early ischemia. We hypothesize, by detecting variations of the IR signal, we can assess the degree to which renal surface temperature reflects underlying renal ischemia. To address this hypothesis, IR imaging-derived temperature fluctuations were evaluated during laparotomy in a porcine model (n = 15). These temperature profiles then underwent spectral (frequency) analysis to assess their relationship to well-described oscillations of the microcirculation.**

Materials and methods. **An IR camera was positioned 30–60 cm above the exposed kidneys. Images (3–5 μm wavelength) were collected (1.0/s) at baseline, during warm renal ischemia, and during reperfusion. Dominant frequency (*DF*) of the tissue temperature fluctuations were determined by a Fourier transformation (spectral) analysis.**

Results. **IR images immediately showed which segments of the kidney were ischemic. *DF* at ~0.008 Hz that corresponds to blood flow oscillations was observed in thermal profiles. The oscillations were diminished or disappeared after 25 min of warm ischemia and were recovered with reperfusion in a time-dependent fashion. Oscillations were attenuated substantially in ischemic segments, but not in perfused segments of the kidney.**

Conclusions. **The described oscillations can be measured noninvasively using IR imaging in the operating room, as represented by the *DF*, and may be an early marker of critical renal ischemia.**

Key Words: **infrared imaging; kidney vasculature; blood flow regulation; and ischemia.**

INTRODUCTION

The determination of organ viability is critical during many operative interventions and specifically plays a crucial role in the assessment of post transplant reperfusion, traumatic devitalization, or resection of ischemic tissues. Currently, operative assessment of organ ischemia is made by subjectively interpreting visual and tactile clues such as color, mottling, and tissue turgor. Objective clinical instrumental approaches, such as fluorescein dye [1] or laser interrogation [2], that focus on the determination of blood flow, are cumbersome and fail to directly characterize ischemic injury. Surrogate serum markers of ischemic injury and histopathology require a significant amount of time following an injury to demonstrate an effect and thus fail to acutely detect an ischemic insult. As such, early objective intraoperative markers of clinically significant critical ischemia, in which permanent damage may occur, are lacking. Importantly, it is at the time of ischemic insult that interventions can preempt irrevocable harm and prevent the cascade of downstream effects seen with ischemia or reperfusion injury [3]. Therefore, an objective method, which is specific to

[1] To whom correspondence and reprint requests should be addressed at Regenerative Medicine, Combat Casualty Care, Naval Medical Research Center, 503 Robert Grant Avenue, Suite 2W123, Silver Spring, MD 20910. E-mail: elstere@nmrc.navy.mil.

[2] Current affiliation: Emory University Hospital, Emory Transplant Center, Atlanta, Georgia.

0022-4804/08 $34.00

ischemic injury and capable of real-time assessment and quantification, is needed.

Based on the principles of thermography, two-dimensional image presentation of natural emission temperature differentials between adjacent structures and assessments of tissue perfusion can be determined in real-time using an advanced digital infrared (IR) camera [4, 5]. Evaporation from the operative field increases heat dissipation, substantially cooling the surface of exposed tissues [6], and amplifies temperature differences between perfused and underperfused tissues, which are readily measurable by IR methods. We have previously shown that these differences can be quantified and used to assess intraoperative cerebral perfusion [7, 8] and to provide real-time assessments of whole kidney reperfusion during renal transplantation [9]. We hypothesize that, by detecting regional and temporal variations of the IR signal, we can assess the degree to which renal surface temperature reflects underlying renal ischemia during laparotomy.

Viable tissues express intrinsic low-frequency oscillations that are believed to represent either an endothelium dependent pacemaker tone [10, 11], myogenic activity of vascular smooth muscle, neurogenic activity of the vessel wall [12], or in the case of the kidney in particular, autoregulation in the form of tubuloglomerular feedback [12–16]. The physiological signals, which are thought to be modulated by vascular endothelium, have been measured with single-point laser Doppler probes in dermal vessels at a frequency of 0.0095 to 0.0100 Hz. While the observation of these intrinsic oscillations has added to the understanding of the physiology of the microcirculation and have been clinically applied to detecting disturbances of the microcirculation in patients with end-stage renal disease, they have not been assessed as a surrogate marker of ischemic injury.

We now show, using whole-organ IR imaging of prolonged renal ischemia in a large animal surgical model, that IR imaging, in addition to detecting tight correlations between temperature and tissue perfusion [5, 7–9], also detects low-frequency oscillations that correlate with critical ischemia. By applying Fourier analysis to IR thermal profiles, we have observed a very low dominant frequency (*DF*) *in vivo* that corresponds to intrinsic blood flow oscillation frequencies. Temperature, rate of temperature change, and extent of *DF* oscillations demonstrated correlations with the duration of controlled ischemia when compared between different experimental conditions (baseline as a control, warm renal ischemia, and reperfusion). Therefore, we believe this *DF* represents an early marker of critical renal ischemia that can be measured noninvasively using real-time IR imaging in the operating room and as such may provide objective assessment of organ viability.

METHODS

Large Animal Renal Warm Ischemia Model

A porcine model of renal ischemia was used to evaluate IR imaging and the degree to which renal surface temperature reflects underlying renal ischemia during laparotomy. Fifteen pigs (2 female, 13 male), between 5 and 9 months of age (23 to 73 kg), were used under an Institutional Animal Care and Use Committee-approved protocol. Animals were maintained following the guidelines issued by the Institute of Laboratory Animals Resources, National Research Council. General anesthesia with 1% isoflurane was administered and laparotomy was performed with bilateral renal mobilization, hilar dissection, and identification of segmental branches on all 15 animals (22 kidneys total). Animals were then divided into two groups: group 1 ($n = 11$) underwent sequential cross-clamping of the entire renal hilum for 10 to 75 min of warm ischemia followed by reperfusion from 5 to 55 min; group 2 ($n = 11$) underwent ligation of a segmental renal vessel (superior or inferior pole) followed by cross-clamping and reperfusion as in group 1.

IR and visible wavelength cameras were positioned 30–60 cm above surgical field to image an entire exposed single kidney ($n = 8$) or pair of kidneys ($n = 7$). Serial field images (320 × 256 pixels each, 1.0/s) of each of the 22 kidneys (10 right and 12 left) were collected during baseline conditions, focal and global ischemia, reperfusion, and post-reperfusion.

The duration of image acquisition for baseline conditions was between 5 and 60 min.

Imaging

An advanced digital IR camera (Infrared Focal Plane Array camera; Lockheed Martin IR Imaging Systems, Inc., Goleta, CA) was used to image local temperature across the exposed kidney by passively detecting IR emission. IR emission at the measured wavelength (3–5 μm) is proportional to temperature, and the calibrated camera was sensitive to 0.02°C temperature changes.

The camera was attached to an operating microscope stand (Zeiss, Gottingen, Germany) and was covered with conventional surgical draping to maintain the sterility of the surgical site. Operative lighting does not influence IR measurements except for those close enough to the exposed kidney to produce local heat. For this reason, surgical lights near the operative site were redirected from the surgical field during the IR measurements.

Sequential digital images were obtained with the detector plane of the IR camera positioned parallel to the plane of the targeted kidney or the central part of the exposed abdomen. The images were displayed on a large (150-cm-diagonal) screen, using a small video projector, and were visible to the surgeon during the procedure. IR image sets for each animal were acquired for 250-600 s with at least 1 min between sets. Images were collected in four separate conditions: (1) after surgical exposure of the kidney (baseline); (2) during the occlusion period (ischemia); (3) after the occlusion was relieved, following removal of the clamp (reperfusion); and (4) during post-reperfusion.

Data Analysis

Successive IR image sets were stored on an Axil Ultima workstation (Axil Computer, Inc., Santa Clara, CA) and analyzed (ENVI/IDL software; ITT Visual Information Solutions, Boulder, CO) postoperatively. A four-step data analysis approach is outlined in Fig. 1. This image analysis was able to identify *DF* oscillations in the temperature profiles, to calculate their spatial extent, to identify oscillations in synthesized images, and to correlate their locations with regions of diminished IR signal triggered by local or global perfusion deficit.

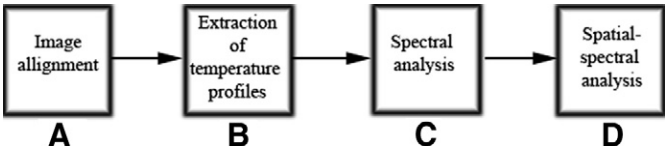

FIG. 1. Four-step data analysis approach. (A) IR images were aligned to remove motion artifacts. The designed image alignment algorithm was applied to a different set of fiducial points until it showed a well-aligned (<5 pixels shift per frame) final image set. (B) Temperature profiles (IR intensity *versus* time) were obtained for the following regions of interest (ROIs): (1) the entire kidney; (2) three standard segmental ROIs (middle, inferior, and superior poles of kidney); and (3) a local ROI (5 × 5 pixels) within each IR frame of an imaging sequence. (C) Spectral analysis was applied to identify the frequency range of temperature profile oscillations extracted from the entire kidney ROI for each baseline trial. A power spectrum was calculated [26] by applying a fast Fourier transformation (FFT) to the 250 points of the data in each thermal profile of each trial. The *DF* was selected from among all thermal profiles and, after linear interpolation across successive trials, the mean *DF* power spectrum for the entire kidney ROI and for local ROI was calculated. (D) Spatial-spectral analysis was performed in two substeps: (a) For each imaging trial, an image was synthesized that gave the color black to those pixels for which the power spectrum magnitude of the *DF* was larger than a chosen threshold (ROI_*DF*). White was assigned to those pixels with magnitudes for *DF* oscillations smaller than the chosen threshold. The threshold was the mean power spectrum for the occluded ROI, plus two times the SD (95% confidence interval). The synthesized image reflected the spatial extent of *DF* oscillations within the kidney. (b) To quantify the spatial extent of *DF* oscillations, the black pixels within the synthesized image were counted for each trial. To minimize the effects of differences in kidney sizes, the counts were normalized by the total number of pixels in the perfused region of kidney (for post-occlusive reactive hyperemia and post-reperfusion conditions) or by the total number of pixels in the entire kidney for baseline and ischemic conditions.

Statistical Analysis

Regression analysis was performed using SigmaStat software (Systat Software, Inc., Richmond, CA) to reveal the relationships between temperature profiles and ischemic conditions, and the extent of *DF* oscillation and ischemic conditions. Slopes and correlations were evaluated using a statistical significance of $P < 0.05$. Multiple comparisons of kidney temperatures, rates of temperature change, normalized power spectra at the *DF*, as well as normalized areas of region of interest (ROI)_*DF* among the different perfusion conditions were performed using a one-way analysis of variance (ANOVA) ($\alpha = 0.05$) followed by the Student—Newman–Keuls test ($\alpha = 0.05$). Normality was tested by a Kolmogorov–Smirnov test while equality of variances was tested by a Levene median test. If one of the latter tests failed, Kruskal–Wallis one-way ANOVA on ranks ($\alpha = 0.05$) was used followed by Dunn's method ($\alpha = 0.05$) of comparison. All values are expressed as means ± SE.

RESULTS

IR Imaging Correlates with Renal Ischemia

Fig. 2 demonstrates the time course of warm renal ischemia in two representative cases: entire left kidney with global ischemia (Fig. 2A) and right kidney with local ischemia (Fig. 2B). IR images and temperature profiles extracted (Fig. 2A and B) showed steady-state variations of the temperature during baseline conditions, gradual cooling during occlusion, dramatic increases in temperature with overshoot after reperfusion (post-occlusive reactive hyperemia, PORH), and post-reperfusion returns of temperature to baseline ($n = 16$). As demonstrated in Fig. 2, regions with diminished pixel intensities corresponded exclusively to regions of global (images *c* and *h*) or regional (image *i*) deficits in renal perfusion ($n = 22$). As the warm ischemia time increased, the temperatures of the entire kidney diminished and the degree of these changes was dependent on the ischemic time (Fig. 3A). For all kidneys studied ($n = 22$), this effect demonstrated a linear relationship for the duration of ischemia ($r^2 = 0.60$, $P < 0.001$) (Fig. 3B).

Renal PORH Correlates with Recovery from Reperfusion

All kidneys studied showed cumulative declines in temperature with increases in ischemic time (Fig. 3). Temperature recoveries were apparent in most kidneys during PORH and post-reperfusion conditions (Fig. 4). IR images demonstrated that, among the 22 kidneys studied, 16 (7 with partial and 9 with total occlusion) showed full postischemic temperature recovery; three with partial occlusion showed limited temperature recovery, and three (including one with partial and two with total occlusion) failed to achieve temperature recovery after ischemia.

For all investigated kidneys the maximum rate of temperature change (arbitrary units/min) was seen during PORH (330.1 ± 38.1, $n = 19$), and the minimum rate was seen at baseline (−1.3 ± 1.3, $n = 22$). Kruskal–Wallis One-Way ANOVA on Ranks was performed ($\alpha = 0.05$). There was a significant difference ($P < 0.001$) for the absolute rate of temperature change among different kidney conditions (baseline, ischemia, PORH, and reperfusion).

Fourier Analysis of Thermal Data Demonstrates a Tissue Intrinsic Dominant Frequency

Detailed analysis of power spectra for IR-derived thermal profiles showed oscillations with a frequency range of 0.004 to 0.020 Hz (Fig. 5). The respiratory component was reduced by a factor of ~10 after image alignment, and the maximum spectral magnitude, the *DF* component, was found to be at ~0.008 Hz.

In an attempt to eliminate the possibility of the *DF* as an instrumental artifact, an additional 18-min imaging session was made by collecting IR images from a black body radiation source. As was done for renal studies, the same detailed analysis of power spectra for IR-derived thermal profiles showed no components in the frequency range of 0.004 to 0.02 Hz. In particular, no maximum spectral magnitude was found near 0.01 Hz. Therefore, we conclude that the finding of a *DF* is a consequence of the renal thermal profiles.

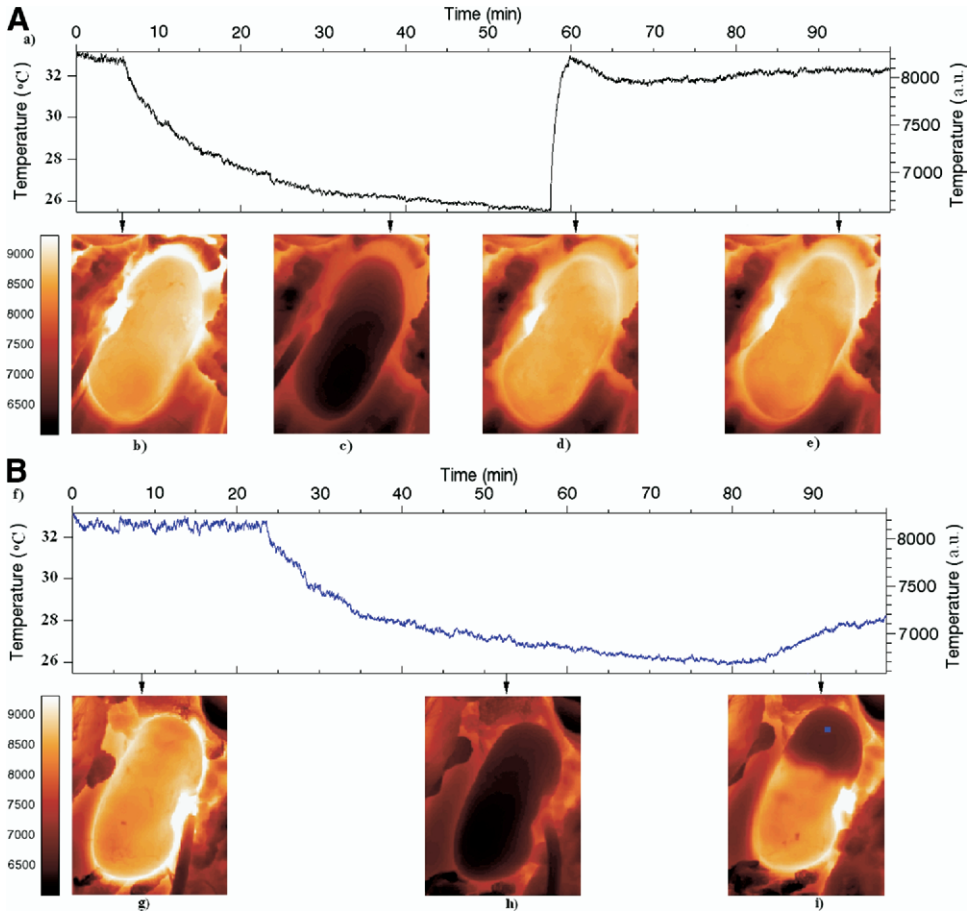

FIG. 2. Representative temperature profiles and IR images during warm renal ischemia. (A) Temperature profile (IR, intensity *versus* time) was plotted from a set of 6000 registered IR images for the left kidney collected over 100 min. The black graph profile (a) was extracted from an entire imaging set collected during baseline (0–6 min), ischemia (6–58 min), post-occlusive reactive hyperemia, PORH (58–65 min), and post-reperfusion (65–100 min) conditions. Four IR images of the left kidney were chosen from among 6000 registered images. Each image (a pseudo-colored intensity map) represents temperature gradients in the kidney parenchyma during baseline (b), ischemia (c), PORH (d), and post-reperfusion (e) for the left kidney. (B) Temperature profile (IR intensity *versus* time) was plotted from a set of 6000 registered IR images for the right kidney collected over 100 min. The profile (f, blue graph) was extracted from a 5 × 5 pixel-square *local* ROI on the kidney's superior pole (i, blue square) during baseline (0–24 min), occlusion (24–80 min), and post-reperfusion (80–100 min) conditions. Three IR images of the right kidney were chosen from among 6000 registered images. Each image (a pseudo-colored intensity map) represents temperature gradients in the right kidney parenchyma during baseline (g), ischemia (h), and post-reperfusion (i). (Color version of figure is available online.)

To eliminate the effect of cardiac pulsation, we used an image alignment algorithm. To verify the quality of this algorithm, first, 5-pixel translational displacement with frequency of 0.008 Hz was added to the experimental IR imaging data set to synthesize a new simulation data set. Extracted from this simulated set, pixel profiles showed a clear *DF* peak at 0.008 Hz before image alignment. Comparison of *DF* spectra extracted from aligned and not-aligned simulated imaging sets showed an ~2 to 3 times (baseline condition) and 10 to 20 times (ischemic condition) suppression of the 0.008 Hz frequency. Next, after image alignment of both original IR and simulated imaging sets, less than a 2% and 10% difference in *DF* power between these sets was found for the baseline and ischemic conditions, respectively. Therefore, it also appears that the *DF* is not related to the data analysis techniques used.

Decreased *DF* Is Associated with Prolonged Renal Ischemia and Is Seen in all Segments of the Kidney

The *DF* power spectra from combined data for all kidneys studied showed a decline in *DF* oscillations up to 25 min following the start of occlusion. After that, the spectral power of the oscillations remained small and almost constant (Fig. 6A). When analyzed as the normalized area of ROI that displays the *DF* (area of entire kidney or area of kidney's inferior/superior pole), the decline in oscillations seen at the 25th min persisted (Fig. 6B).

Furthermore, as compared with Fig. 4, the extent of PORH measured using the *DF* is more dramatic than measured using IR imaging (Fig. 7). When ROIs were analyzed according to anterior segmental perfusion (superior, middle, and inferior based on vascular sup-

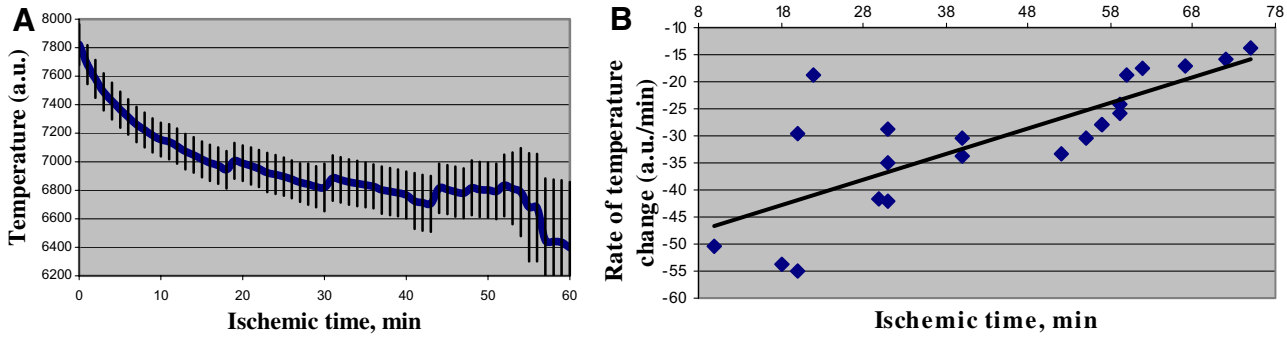

FIG. 3. Dependency of kidney temperature and rate of temperature change on warm ischemia time. (A) The mean and standard error of the temperature profile (entire kidney ROI) during the kidney occlusion ($n = 22$). (B) Rate of temperature change (in arbitrary units/min; entire kidney ROI) during occlusion *versus* ischemic time. Regression analysis: $y = -51.5 + 0.477*x$, $r^2 = 0.60$, $P < 0.001$, $n = 22$. (Color version of figure is available online.)

ply), there was no segmental differences measured with either IR or *DF* (data not shown).

DF Is Demonstrated in Reperfused Regions of the Kidney

Image analysis demonstrated *DF* oscillations were attenuated substantially in ischemic segments, but not in perfused segments of the kidney. During ischemic conditions in all kidneys receiving at least 25 min of *partial* or *total* occlusion, the synthesized images showed no temperature oscillations, or only limited extent of oscillations (approximately 10% of total renal area). During PORH, the synthesized images of 16 kidneys showed oscillations in reperfused areas only. For kidneys that failed to achieve temperature recovery during reperfusion (one with partial and two with *total* occlusion), no oscillations were manifested during PORH. For three kidneys with partial occlusion and limited temperature recovery, it was possible to see a limited extent of oscillations in the reperfused region of the kidney, and even then only at a lower level of statistical significance. These effects are demonstrated in Figs. 8 and 9. The degree of recovery of the *DF* after reperfusion, as represented by the % *DF*, was inversely proportional to the length of the warm ischemia period as demonstrated in Fig. 10.

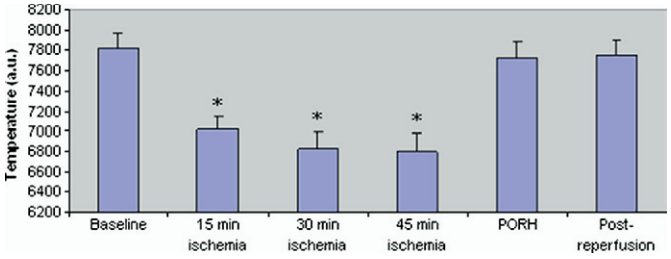

FIG. 4. Temperature fluctuations during ischemia and reperfusion. Temperature fluctuations for different kidney conditions and ischemic times, shown at baseline ($n = 22$), 15 min of ischemia ($n = 21$, entire kidney ROI), 30 min of ischemia ($n = 17$, entire kidney ROI), 45 min of ischemia ($n = 11$, entire kidney ROI), post-occlusive reactive hyperemia, PORH ($n = 16$, perfused ROI), and post-reperfusion ($n = 16$, perfused ROI). ANOVA was performed ($\alpha = 0.05$). When compared to baseline, there was a significant difference at 15, 30, and 45 min of ischemia and no significant differences at PORH and post-reperfusion. *Significant difference ($P < 0.05$) *versus* baseline. (Color version of figure is available online.)

DISCUSSION

The ability to precisely determine the degree of ischemia of a particular tissue at the operating table has wide applicability to many surgical disciplines including solid organ transplantation, trauma, and nephron-sparing surgery [17–20]. In these and many other instances, the ability to objectively determine organ viability could be expected to acutely alter surgical decision-making and guide more precise operative intervention. The data reported herein demonstrate a method, available in the operating room, for immediate recognition of ischemic tissue. We have studied this in renal warm ischemia.

In this series of experiments the thermal profiles of renal ischemia correlate with the degree of warm ischemia (Fig. 3) and demonstrate the degree of reperfusion and the ability of the organ to recover (Fig. 4). Fourier analysis of these thermal profiles demon-

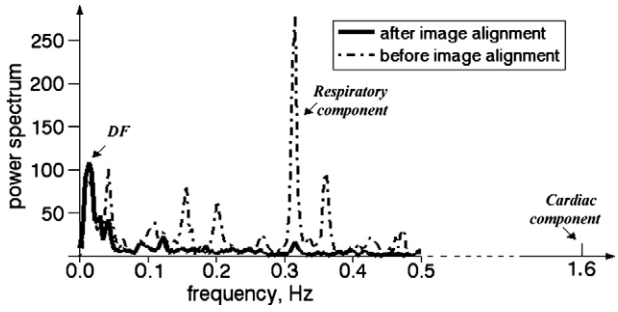

FIG. 5. IR oscillations before and after image alignment. Frequency components of thermal profiles revealed in power spectrum, before (dashed line) and after (solid line) image alignment. Note the respiratory (~0.29 Hz) and dominant frequency, *DF* (0.008 Hz), frequency components. Note that a synthesized cardiac-related component (~1.6 Hz) is shown here for reference purposes.

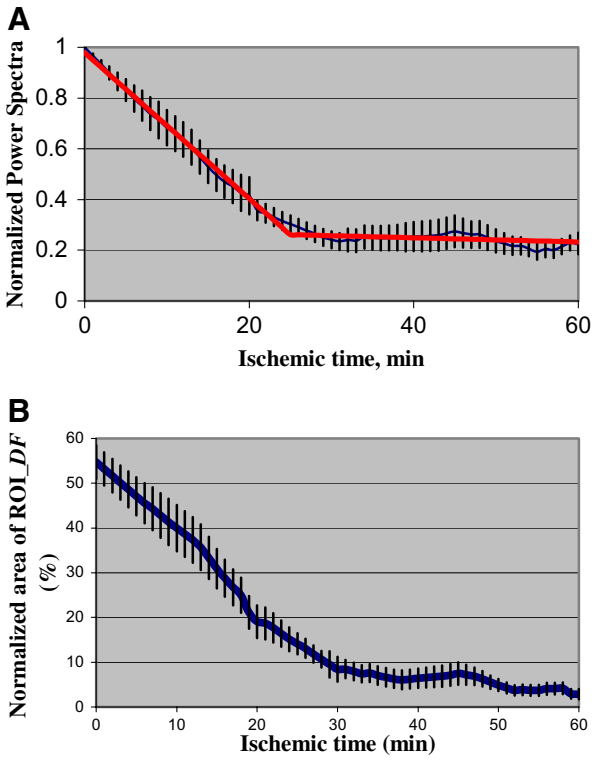

FIG. 6. Dependency of power spectra for entire kidney and ROIs that display the *DF* during warm ischemia. (A) *DF* power spectra for entire kidney ROI thermal profiles from IR images collected during ischemia (n = 22). Data were normalized to baseline power spectra. A two-segment piecewise linear regression fit (red line) was used. The breakpoint (the transition point of these two estimated linear segments) is at the 25th min. (B) The normalized area of ROI_*DF versus* ischemic time (n = 22). (Color version of figure is available online.)

strates a *DF* (Fig. 5) which is thought to represent intrinsic renal oscillations, and these oscillations disappear at 25 min of warm ischemia, a critical time point as discussed above (Fig. 6). These oscillations are also shown to recover with reperfusion, dependent on the length of the warm ischemia period (Figs. 7–10). Taken together, these findings suggest that thermal imaging not only can assess renal perfusion, but also allows for the determination of the *DF* that represents intrinsic oscillations and may be a surrogate marker for critical ischemia.

The presence of intrinsic oscillations in both kidney and skin is well documented and is thought to represent either tubuloglomerular feedback or a regulatory mechanism of the microvascular circulation [12, 14, 21, 22]. Kidney-specific oscillations are thought to control renal blood flow via tubuloglomerular feedback and occur at a frequency of 0.033 Hz in rats [14–16, 23, 24] and ~0.025 Hz in dogs [13]. Very low-frequency oscillations at wavelengths similar to those demonstrated in the present study have also been reported in the skin and speculated to represent an endothelial dependent pacemaker [11, 12]. While oscillations at frequency of 0.01 Hz are thought to be mediated by nitric oxide, those at frequencies lower than this (such as the *DF* observed in this set of experiments) are not dependent on nitric oxide and are thought to be related to the endothelial-derived hyperpolarizing factor [11]. As such, they have been evaluated as a noninvasive tool to diagnose disturbances of the microcirculation as seen in patients with endothelial cell dysfunction secondary to end-stage renal disease and diabetes mellitus. The finding of similar frequency oscillations in the renal parenchyma is not surprising, as the mechanisms behind endothelial cell communication are likely preserved throughout all organ systems. However, their assessment with thermal imaging and the association with warm ischemia are two novel findings. If these oscillations are indeed preserved throughout the endothelium, then the assessment of tissue ischemia in any organ may be amenable to this type of noninvasive evaluation.

To validate the presence of these oscillations, we performed measurements using a black body radiation source and detected no *DF*. We did however detect the presence of cardiac noise that can be attributed to at least two mechanisms: cardiac inflow and pulsation. Although the 1-Hz sampling rate under-sampled the cardiac inflow effect and may produce an aliasing (distortion or artifact) signal, the cardiac spectra would fold over into the frequency around the 0.4 Hz instead of the *DF*. In our study this aliased spectral component was negligible (<5%) when compared with the *DF* spectra. This indicates that even cardiac aliased noise under a *Nyquist* frequency of 0.5 Hz may have occurred but did not impose a significant confounding factor for our measurements. In addition we have demonstrated that the imaging alignment algorithm itself suppressed tissue displacement effects successfully and

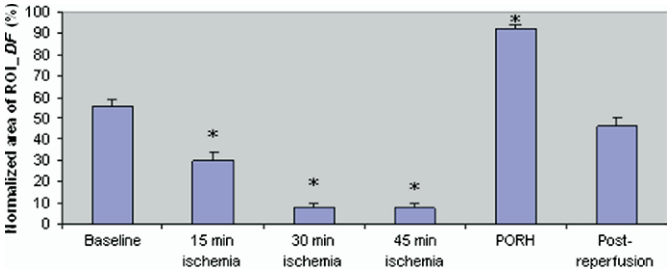

FIG. 7. Spatial extent of *DF* oscillations during ischemia and reperfusion. Spatial extent of oscillations (% of black pixels normalized to area of entire kidney or area of kidney's inferior/superior pole) for different conditions: baseline (n = 22), 15 min of ischemia (n = 21), 30 min of ischemia (n = 17), 45 min of ischemia (n = 11), post-occlusive reactive hyperemia, PORH (n = 16), and post-reperfusion (n = 16). ANOVA was performed (α = 0.05). When compared to baseline, there was a significant difference at 15, 30, and 45 min of ischemia and PORH. There was no significant difference at post-reperfusion. *Significant difference ($P < 0.05$) *versus* baseline. Normalized area of ROI_*DF* = (area of ROI_*DF*)/(area of entire kidney or area of kidney's inferior/superior pole). ROI, regions of interest. (Color version of figure is available online.)

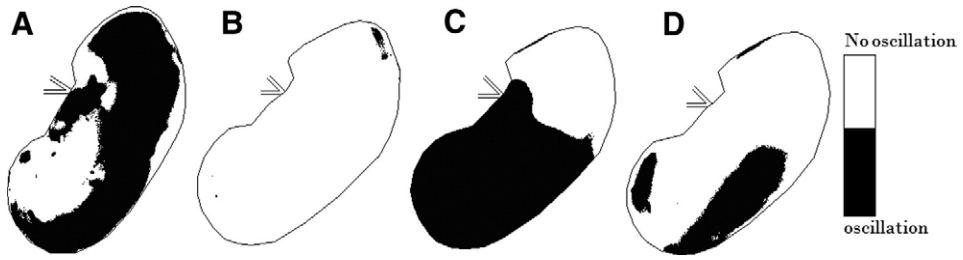

FIG. 8. Representative distribution of *DF* oscillations. Representative distribution of *DF* oscillations in renal IR images during (A) baseline, (B) ischemia, (C) post-occlusive reactive hyperemia, PORH (following partial occlusion), and (D) post-reperfusion (following partial occlusion).

therefore the *DF* was not produced by the image alignment procedure or translational tissue movement.

A generally acceptable upper limit of renal warm ischemia of 30 to 45 min was established based on experiments done in the 1970s, although more recent animal models suggest that this window may be extended up to 90 min in the nontransplant population [18, 19]. Multivariate analysis of risk factors associated with early graft failure in patients receiving non-heart-beating (NHB) kidneys clearly identifies 30 min of warm ischemia as a significant risk factor [18]. Smaller case series of NHB renal transplant recipients substantiate this time limitation; however, the effect was not uniform in that some organs with greater than 30 min of warm ischemia did function well in both the short and the long term [17, 18]. In addition, large animal models in which uni-nepheric animals are subjected to prolonged warm ischemia demonstrate full recovery with warm ischemia times twice that seen in NHB donors [19]. Although these models are not identical (*in situ* warm ischemia *versus* transplantation of NHB organs), they do highlight the current limitations in both the assessment of warm ischemia and the limits of warm ischemia.

While objective clinical parameters to assess warm ischemia are not currently used, several methodologies have been studied in small animal models to assess renal ischemia. One promising method reported is the use of optical spectroscopy to assess auto-fluorescence intensity of nicotinamide adenine dinucleotide dehydrogenase to determine tissue hypoxia coupled with light scattering to measure cellular and molecular tissue changes with ischemia. When analyzed together, these complementary optical spectroscopy methods provide an assessment of warm ischemia in a rodent model [25]. Similar to our IR approach, optical spectroscopy provides a whole field assessment of the organ of interest, allowing for determination of heterogeneity and real-time feedback. However, this technology has been limited by the need for and the amount of tissue penetration achieved by laser excitation (100 μm), therefore making this an ideal research tool for small animal studies but impractical for humans or larger animals in which the renal capsule is much thicker. IR provides much deeper tissue assessment while remaining a passive camera, therefore not requiring external sources of energy such as lasers used in this and other methods. These characteristics, coupled with the current ease of intraoperative use of IR cameras in clinical settings, make this an ideal imaging approach that can be transferred to clinical use with minimal intrusiveness [9] Furthermore, efforts are underway to expand IR

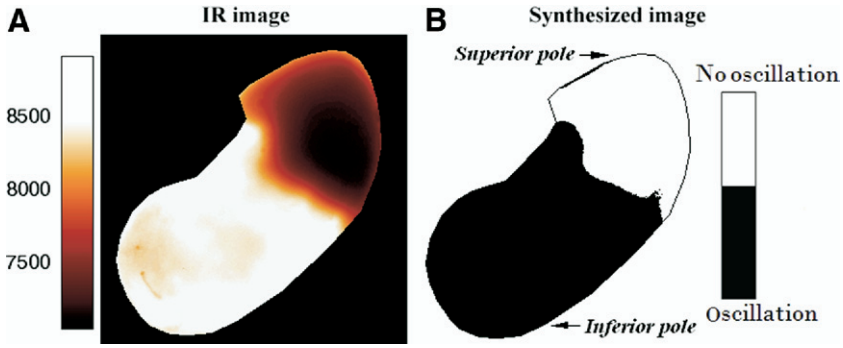

FIG. 9. IR image (A) and synthesized image (B) of the same kidney during PORH. IR image (A) and synthesized image (B) of the same kidney during PORH. This is a representative case in which the blood supply to the left kidney's superior pole is interrupted by a permanent clip prior to total occlusion of blood to the kidney by a temporary hilar clamp. After 47 min of ischemia to the entire kidney, the hilar clamp was removed. The IR image shown here was taken 2.2 min later. The synthesized image reflects the spatial extent of oscillations (one oscillation per 2.08 min). A total of 35,230 thermal profiles were extracted from 250 IR images (during PORH), and a *DF* of 0.008 Hz was identified in the power spectrum. Note that the same kidney segment (superior pole) appears under-perfused (IR image, dark red color) and has no oscillations in the synthesized image (white color). (Color version of figure is available online.)

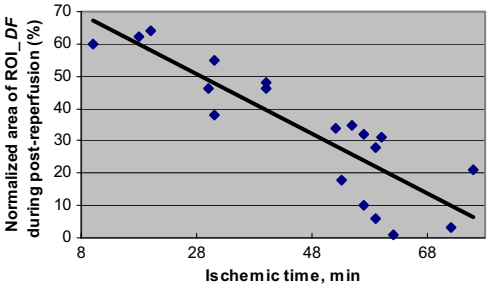

FIG. 10. Spatial extent of oscillations *versus* ischemic time. Spatial extent of oscillations (% of pixels with *DF* oscillation normalized to area of entire kidney or area of kidney's inferior/superior pole) *versus* ischemic time. Data are analyzed for 4.2 min of post-reperfusion starting from PORH maximum ($n = 19$). Regression analysis: $y = 76.4 - 0.92*x$, $r^2 = 0.75$, $P < 0.001$, $n = 19$ (only animals with PORH and with limited recovery are reflected). Normalized area of ROI_*DF* = (area of ROI_*DF*)/(area of entire kidney or area of kidney's inferior/superior pole). For full kidney occlusion, it is normalized by the area of the entire kidney. For partial kidney occlusion, it is normalized by the area of the kidney's inferior or superior pole. Data are normalized by the area of the entire kidney for total kidney occlusion and normalized by the area of the kidney's inferior or superior pole for partial kidney occlusion. (Color version of figure is available online.)

imaging beyond open surgery by the development of IR-capable laparoscopes that will extend the capability to assess organ ischemia to minimally invasive operations such as laparoscopic donor nephrectomy and laparoscopic partial nephrectomy, in which assessment of tissue ischemia is critical.

The major limitation of our current approach is the prolonged time required for image acquisition during which external movement must be minimized. We are developing computational algorithms that compress the acquisition time down to 4 to 5 min, extrapolate the *DF* from this collection period, and provide real-time feedback to the surgeon in a fashion that is clinically useful. In addition, as intraoperative IR allows for a depth of interrogation at this *DF* of about 1 to 2 cm, these observations represent cortical changes and may not reflect alterations in deeper structures. Finally, while we have demonstrated that the *DF* is associated with warm ischemia, we have not addressed the association between recovery of the *DF* and return of renal function. However, as the limits of warm renal ischemia established in both animal and clinical studies fall within the time period of 25 min, the correlation of the *DF* and renal ischemia appears valid. Studies are currently underway to correlate the findings presented herein with functional recovery that will allow for transition of this approach to the clinic.

In summary, we have demonstrated the ability to assess gross and focal deficits in renal perfusion using IR intensity imaging in a large animal model of warm ischemia. IR imaging immediately showed which segments of the kidney were occluded or perfused, and correlated with prolonged ischemia times. Spectral analysis of the temperature profiles obtained for segmental and local regions-of-interests demonstrated low frequency blood flow oscillations (the *DF*), which were attenuated substantially in ischemic segments but not in perfused segments of the kidney. In addition, the *DF* became attenuated at 25 min of warm ischemia, a time point associated with functional impairment in renal transplantation, and recovered during reperfusion in a time-dependent fashion. We believe these oscillations represent local vasomotion and endothelial damage at the site of ischemia and may be broadly applicable to all forms of end-organ ischemia. This phenomenon may be useful for the *in vivo* assessment of ischemic injury and endothelial cell integrity in real-time and may represent an early marker of critical renal ischemia, thereby providing objective evidence to expand the use of marginal organs, allow for more aggressive nephron-sparing surgery, and provide objective evidence for renal salvage after traumatic injuries.

ACKNOWLEDGMENTS

The authors would like to acknowledge the significant contributions of Mehrdad Alemozaffar, B.S., Neil Kansal, M.D., Doug K. Tadaki, Ph.D. to the implementation and support of this study. The authors would like to thank Henry Eden, M.D., Ph.D., for his invaluable critique and insightful comments during preparation of this manuscript.

This work was supported by the intramural research funds of National Institutes of Health and Department of Defense (work unit number: 602227D.0483.01.A0518, Medical Free Electron Laser program).

REFERENCES

1. Horgan PG, Gorey TF. Operative assessment of intestinal viability. Surg Clin North Am 1992;72:143.
2. Ando M, Ito M, Nihei Z, Sugihara K. Assessment of intestinal viability using a non-contact laser tissue blood flowmeter. Am J Surg 2000;180:176.
3. Schlichting CL, Schareck WD, Weis M. Renal ischemia-reperfusion injury: New implications of dendritic cell-endothelial cell interactions. Transplant Proc 2006;38:670.
4. Gorbach AM. Infrared imaging of brain function. Adv Exp Med Biol 1993;333:95.
5. Watson JC, Gorbach AM, Pluta RM, et al. Real-time detection of vascular occlusion and reperfusion of the brain during surgery by using infrared imaging. J Neurosurg 2002;96:918.
6. Sessler DI. Perioperative heat balance. Anesthesiology 2000;92:578.
7. Gorbach AM, Heiss J, Kufta C, et al. Intraoperative infrared functional imaging of human brain. Ann Neurol 2003;54:297.

8. Gorbach AM, Heiss JD, Kopylev L, et al. Intraoperative infrared imaging of brain tumors. J Neurosurg 2004;101:960.
9. Gorbach A, Simonton D, Hale DA, et al. Objective, real-time, intraoperative assessment of renal perfusion using infrared imaging. Am J Transplant 2003;3:988.
10. Kvernmo HD, Stefanovska A, Kirkeboen KA, et al. Oscillations in the human cutaneous blood perfusion signal modified by endothelium-dependent and endothelium-independent vasodilators. Microvasc Res 1999;57:298.
11. Kvandal P, Landsverk SA, Bernjak A, et al. Low-frequency oscillations of the laser Doppler perfusion signal in human skin. Microvasc Res 2006;72:120.
12. Stewart J, Kohen A, Brouder D, et al. Noninvasive interrogation of microvasculature for signs of endothelial dysfunction in patients with chronic renal failure. Am J Physiol Heart Circ Physiol 2004;287:H2687.
13. Just A. The mechanisms of renal blood flow autoregulation. Dynamics and contributions. Am J Physiol Regul Integr Comp Physiol 2007;292:R1.
14. Marsh DJ, Sosnovtseva OV, Pavlov AN, et al. Frequency encoding in renal blood flow regulation. Am J Physiol Regul Integr Comp Physiol 2005;288:R1160.
15. Holstein-Rathlou NH, Marsh DJ. A dynamic model of the tubuloglomerular feedback mechanism. Am J Physiol 1990;258(5 Pt. 2):F1448.
16. Holstein-Rathlou NH. Oscillations and chaos in renal blood flow control. J Am Soc Nephrol 1993;4:1275.
17. Gurkan A, Kacar SH, Varilsuha C, et al. Non-heart-beating donors: is it worthwhile? Ann Transplant 2005;10:20.
18. Keizer KM, de Fijter JW, Haase-Kromwijk BJ, et al. Non-heart-beating donor kidneys in the Netherlands: allocation and outcome of transplantation. Transplantation 2005;79:1195.
19. Laven BA, Orvieto MA, Chuang MS, et al. Renal tolerance to prolonged warm ischemia time in a laparoscopic versus open surgery porcine model. J Urol 2004;172(6 Pt. 1):2471.
20. Sangthong B, Demetriades D, Martin M, et al. Management and hospital outcomes of blunt renal artery injuries: analysis of 517 patients from the National Trauma Data Bank. J Am Coll Surg 2006;203:612.
21. Segal SS. Regulation of blood flow in the microcirculation. Microcirculation 2005;12:33.
22. Raghavan R, Chen X, Yip KP, et al. Interactions between TGF-dependent and myogenic oscillations in tubular pressure and whole kidney blood flow in both SDR and SHR. Am J Physiol Renal Physiol 2006;290:F720.
23. Holstein-Rathlou NH, Marsh DJ. Renal blood flow regulation and arterial pressure fluctuations: a case study in nonlinear dynamics. Physiol Rev 1994;74:637.
24. Marsh DJ, Sosnovtseva OV, Chon KH, et al. Nonlinear interactions in renal blood flow regulation. Am J Physiol Regul Integr Comp Physiol 2005;288:R1143.
25. Fitzgerald JT, Demos S, Michalopoulou A, et al. Assessment of renal ischemia by optical spectroscopy. J Surg Res 2004; 122:21.
26. Stoica P, Moses R. Introduction to Spectral Analysis. Englewood Cliffs, NJ: Prentice-Hall, 1997.